## Article:

# Natural aerosol direct and indirect radiative effects

Alexandru Rap,[1] Catherine E. Scott,[1] Dominick V. Spracklen,[1] Nicolas Bellouin,[2] Piers M. Forster,[1] Kenneth S. Carslaw,[1] Anja Schmidt,[1] and Graham Mann[1,3]

[1] Natural aerosol plays a significant role in the Earth's system due to its ability to alter the radiative balance of the Earth. Here we use a global aerosol microphysics model together with a radiative transfer model to estimate radiative effects for five natural aerosol sources in the present-day atmosphere: dimethyl sulfide (DMS), sea-salt, volcanoes, monoterpenes, and wildfires. We calculate large annual global mean aerosol direct and cloud albedo effects especially for DMS-derived sulfate ($-0.23$ Wm$^{-2}$ and $-0.76$ Wm$^{-2}$, respectively), volcanic sulfate ($-0.21$ Wm$^{-2}$ and $-0.61$ Wm$^{-2}$) and sea-salt ($-0.44$ Wm$^{-2}$ and $-0.04$ Wm$^{-2}$). The cloud albedo effect responds nonlinearly to changes in emission source strengths. The natural sources have both markedly different radiative efficiencies and indirect/direct radiative effect ratios. Aerosol sources that contribute a large number of small particles (DMS-derived and volcanic sulfate) are highly effective at influencing cloud albedo per unit of aerosol mass burden. **Citation:** Rap, A., C. E. Scott, D. V. Spracklen, N. Bellouin, P. M. Forster, K. S. Carslaw, A. Schmidt, and G. Mann (2013), Natural aerosol direct and indirect radiative effects, *Geophys. Res. Lett.*, *40*, doi:10.1002/grl.50441.

## 1. Introduction

[2] Atmospheric aerosol is derived from both natural and anthropogenic sources. Natural sources include primary emissions of desert dust, sea-salt, and wildfire aerosol along with aerosol precursors such as sulfur- and carbon-containing gases from vegetation, ocean biology, and volcanoes that can subsequently form particles in the atmosphere [e.g., *Carslaw et al.*, 2010; *Mahowald et al.*, 2011]. Aerosol affects the Earth's radiative balance through the scattering and absorption of shortwave (SW) and longwave (LW) radiation (the aerosol direct effect) and through influencing the formation and properties of clouds, altering both cloud albedo (first indirect or cloud albedo effect) and cloud lifetime (second indirect effect) [*Forster et al.*, 2007].

[3] The role of natural aerosol in affecting the Earth's radiative balance is poorly constrained, with the radiative effects for several important natural aerosol sources still not quantified [*Mahowald et al.*, 2011]. This contributes to poor understanding of natural aerosol interactions and feedbacks within the Earth system [*Carslaw et al.*, 2010].

Furthermore, natural aerosol contributes to aerosol background concentrations [*Andreae*, 2008], the quantification of which is a prerequisite for accurate assessments of impacts of anthropogenic aerosol on clouds and climate [*Menon et al.*, 2002; *Schmidt et al.*, 2012].

[4] Here we explore the role of natural aerosol sources in the Earth system by quantifying the contribution of five natural sources, dimethyl sulfide (DMS) from ocean phytoplankton, sea-salt, wildfires, volcanoes, and monoterpenes from vegetation, to present day (PD) aerosol. We quantify the impact of each natural aerosol source on the Earth's radiative balance. We restrict the use of radiative forcing (RF) to a change in the top-of-atmosphere (TOA) radiative balance relative to preindustrial (PI) conditions [*Forster et al.*, 2007] and we express the impact of natural aerosol to the PD atmosphere as a radiative effect (RE), defined to be the TOA change in radiation due to a change in that natural aerosol source.

## 2. Methodology

### 2.1. Global Aerosol Model

[5] We simulated aerosol concentrations using the GLOMAP-mode global aerosol microphysics model [*Mann et al.*, 2010] at a horizontal resolution of $2.8° \times 2.8°$ driven by European Centre for Medium-Range Weather Forecasts reanalysis data. The aerosol size distribution is treated using a two-moment modal scheme with 5 modes: hydrophilic nucleation, Aitken, accumulation and coarse modes and non-hydrophilic Aitken mode. Within each mode the different aerosol components are internally mixed. New particle formation is simulated through binary-homogeneous nucleation of sulfuric acid and water [*Mann et al.*, 2010]. Natural emissions include oceanic DMS calculated using the DMS sea surface concentration database of *Kettle and Andreae* [2000] along with the sea-to-air transfer velocity of *Nightingale et al.* [2000], passive volcanic degassing and time-averaged explosive $SO_2$ from *Dentener et al.* [2006], sea-salt calculated using the scheme of *Gong* [2003], monoterpenes from *Guenther et al.* [1995], and biomass burning emissions from *van der Werf et al.* [2004]. The importance of humans in altering global fire patterns and the amount of fire in prehuman times is poorly understood [*Bowman et al.*, 2009]. Therefore, in this study we do not distinguish between natural and anthropogenic fire, and estimate upper limit effects by implicitly assuming that all fire is natural. We also assumed that monoterpenes form secondary organic aerosol (SOA) with a fixed yield as detailed in *Mann et al.* [2010] and carbonaceous aerosol is emitted using the initial size distribution from *Stier et al.* [2005]. We assume that non-hydrophilic aerosol may be physically aged by one monolayer of condensable material (secondary organics or sulphuric acid), and transferred

---

[1]School of Earth and Environment, University of Leeds, Leeds, UK.
[2]Department of Meteorology, University of Reading, Reading, UK.
[3]National Centre for Atmospheric Science, Leeds, UK.

Corresponding author: A. Rap, School of Earth and Environment, University of Leeds, Leeds, UK. (a.rap@leeds.ac.uk)

**Table 1.** Annual Global Mean Aerosol Burden, Optical Depth at 0.55 μm, Contribution to CDNC at Cloud Base, Direct and Indirect Radiative Effects, Burden and AOD Clear-Sky Radiative Efficiencies[a]

| | Study | Burden[b] [mg m$^{-2}$] | AOD at 0.55 μm | ΔCDNC [%] | Clear-Sky Direct RE [W m$^{-2}$] | All-Sky Direct RE [W m$^{-2}$] | Indirect RE [W m$^{-2}$] | DRE Burden eff.[c] [W/g] | DRE AOD eff.[d] [Wm$^{-2}$/τ] | CAE Burden eff.[c] [W/g] |
|---|---|---|---|---|---|---|---|---|---|---|
| PD-PI | This | 2.58 | 0.032 | | −0.82 | −0.46 | −0.95 | −318 | −26 | −368 |
| | Prev. | 3.7±0.9[h] | 0.029±0.01[h] | | −0.68± 0.24[h] | −0.22±0.16[h]; [−0.9,−0.1][o] | [−1.8,−0.3][o]; −1.8[l] | | −23±7[h] | |
| DMS sulfate | This | 0.57 | 0.010 | 10.2 | −0.35 | −0.23 | −0.76 | −616 | −35 | −1336 |
| | Prev. | 0.39[j] | | | | −0.17[j] | e,f-2.03[n] | | | |
| Sea-salt | This | 8.87 | 0.019 | 1.3 | −0.70 | −0.44 | −0.04 | −79 | −36 | −4.9 |
| | Prev. | (7.5–36.8)[k] 9.2[i];7.6[l] | 0.027[i] | | (−1.5,−5)[k]; −0.42[i] | −0.18[i] | −1.82[l] | −46[i] | | −239[l] |
| Volcanic sulfate | This | 0.69 | 0.008 | 9.2 | −0.30 | −0.21 | −0.61 | −430 | −35 | −892 |
| | Prev. | 0.72[q]; 0.56[j] | | 9.4[q] | | −0.21[j] | −0.56[q] | | | |
| Terpene SOA | This | 0.25 | 0.003 | 2.4 | −0.14 | −0.13 | −0.02 | −554 | −54 | −101 |
| | Prev. | 0.14[m]; 1.55[p] | | | −0.29[p] | −0.01[m] | g,f-0.19[m] | | | −2753[m] |
| Wildfire | This | 0.6 | 0.004 | 5.3 | −0.06 | −0.01 | −0.09 | −101 | −14 | −151 |
| | Prev. | 0.98[r] | 0.006[r] | | −0.27[r] | 0.13[r] | −1.64[r] | −275 | −45 | |

[a]Our indirect REs only include the CAE, whereas previous work may include additional aerosol cloud effects (see table footnotes). [b]Aerosol burden (e.g., SO$_4$, organic matter). [c]Normalized RE by aerosol burden. [d]Normalized RE per unit AOD. [e]Includes the direct effect. [f]Includes the cloud lifetime effect. [g]Includes semidirect effect. [h]*Schulz et al.* [2006]. [i]*Reddy et al.* [2005]. [j]*Graf et al.* [1997]. [k]*Haywood et al.* [1999]. [l]*Menon et al.* [2002]. [m]*Goto et al.* [2008]. [n]*Thomas et al.* [2010]. [o]*Forster et al.* [2007]. [p]*O'Donnell et al.* [2011]. [q]*Schmidt et al.* [2012] (does not include time-averaged SO$_2$ emissions from explosive eruptions). [r]*Ward et al.* [2012].

to the corresponding hydrophilic mode. We do not calculate the radiative effect of mineral dust.

[6] All model simulations were completed using meteorology for the year 2000 after a 3 month model spin-up. For each natural aerosol source we simulated source strengths of 0%, 25%, 50%, 75%, 90%, and 100%. These simulations included anthropogenic aerosol emissions for the year 2000 according to *Dentener et al.* [2006]. To compare natural and anthropogenic aerosol we completed an additional simulation using PI (year 1750) anthropogenic emissions [*Dentener et al.*, 2006]. We note that *Dentener et al.* [2006] apply different wildfire emissions in 1750, meaning that our anthropogenic RF includes some influence from changing wildfire.

### 2.2. The Radiative Transfer Model

[7] We used the off-line version of the *Edwards and Slingo* [1996] radiative transfer model with 6 bands in the SW and 9 bands in the LW, with a delta-Eddington 2 stream scattering solver at all wavelengths. We employed a monthly mean climatology for water vapor, temperature and ozone based on European Centre for Medium-Range Weather Forecasts reanalysis data, together with surface albedo and cloud fields from the International Satellite Cloud Climatology Project (ISCCP-D2) [*Rossow and Schiffer*, 1999] for the year 2000. The sensitivity of our RE estimates to the cloud climatology was found to be small, according to an extra set of calculations performed using the 1983–2008 multiannual ISCCP cloud climatology (see Table A1 in the auxiliary material).

[8] To estimate the aerosol direct radiative forcing (DRF) and effect (DRE), the radiative transfer model was used along with output from GLOMAP-mode. For each spectral band and all aerosol modes we calculated aerosol optical properties as described in *Bellouin et al.* [2013]. The aerosol DRF and DREs were calculated as the difference of TOA net (SW +LW) radiative fluxes between the PD control and 26 perturbed experiments, i.e., one corresponding to PI conditions and 25 experiments corresponding to 5 different source strengths

(0%, 25%, 50%, 75%, and 90%) for each of the five natural aerosol sources considered. The same perturbed experiments were used to estimate the aerosol cloud albedo forcing (CAF) and effect (CAE) as described in previous studies [*Spracklen et al.* 2011a, 2011b; *Schmidt et al.* 2012]. We calculated cloud droplet number concentration (CDNC) using the mechanistic parameterisation of cloud drop formation [*Nenes and Seinfeld*, 2003] assuming a cloud updraft velocity of 0.2 m s$^{-1}$ as used in *Spracklen et al.* [2011a]. We did not simulate changes to cloud lifetime.

### 3. Results and Discussion

[9] We first present results of anthropogenic RF against which we later contrast the RE from natural aerosol sources. The annual mean anthropogenic aerosol burden, aerosol optical depth at 0.55 μm (AOD), and all-sky net DRF and CAF are illustrated in Figure 1a, with annual global mean values shown in Table 1. Our results compare well with the AeroCom [*Schulz et al.*, 2006] results: anthropogenic AOD of 0.032 (AeroCom mean 0.029±0.01), clear-sky DRF of −0.82 W m$^{-2}$ (AeroCom −0.68±0.24 W m$^{-2}$), all-sky net DRF −0.46 W m$^{-2}$ (AeroCom −0.22±0.16 W m$^{-2}$), and DRF AOD clear-sky efficiency, defined as the TOA clear-sky RF per unit of AOD, of −26 W m$^{-2}$ (AeroCom −23±7 W m$^{-2}$). Our annual global mean CAF estimate of −0.95 W m$^{-2}$ is within the range of previous studies [*Forster et al.*, 2007]. The zonal distributions of DRF and CAF exhibit maxima at around 30°N, matching the anthropogenic aerosol burden (Figure 1 and Auxiliary Material Figure A1a).

[10] Figures 1b–1f show the annual mean REs calculated as the difference between the PD control and complete removal experiments for each natural aerosol source, with annual global mean values reported in Table 1. The spatial patterns of DRE typically match those of the aerosol burden, with the largest DRE over the oceans for both sea-salt and DMS-derived sulfate and over the continents for terpene-derived SOA. In our model, sea-salt is the natural aerosol with the largest global annual mean all-sky DRE calculated as −0.44 W m$^{-2}$. The clear-sky DRE we calculate due to
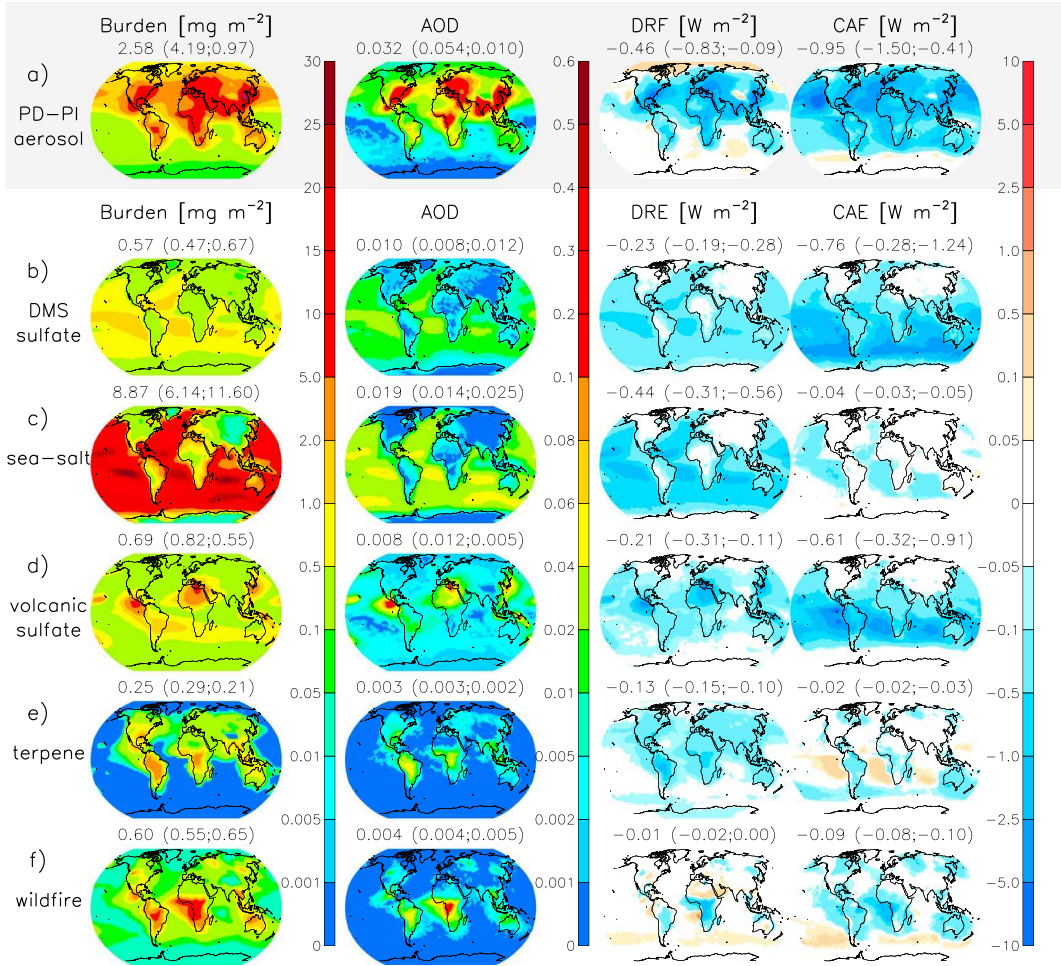
**Figure 1.** Annual mean all-sky aerosol burden, aerosol optical depth at 0.55 μm, direct and cloud albedo net radiative (a) forcing and (b–f) effect for anthropogenic (Figure 1a) and natural aerosol sources (Figures 1b–1f) in the present day atmosphere. Values above each panel are global means, with values in brackets showing Northern and Southern Hemisphere means, respectively.

sea-salt (–0.7 W m$^{-2}$) is at the lower magnitude end of previous studies (–0.42 to –5 W m$^{-2}$) [*Haywood et al.* 1999; *Reddy et al.*, 2005] at least partly due to our low sea-salt mass burden (8.9 mg m$^{-2}$) in comparison to these studies (range 7.5–36 mg m$^{-2}$). We calculate an all-sky DRE for DMS- and volcanic-derived sulfate of –0.23 W m$^{-2}$ and –0.21 W m$^{-2}$, respectively, both agreeing well with the values reported by *Graf et al.* [1997]. We simulate an all-sky DRE from monoterpene derived SOA of –0.13 W m$^{-2}$, which is substantially larger than that calculated by *Goto et al.* [2008] (–0.01 W m$^{-2}$), partly due to the greater SOA burden in our model. Our clear-sky DRE from monoterpene SOA (–0.14 W m$^{-2}$) is smaller than that reported by *O'Donnell et al.* [2011] (–0.29 W m$^{-2}$) who treated SOA from both monoterpene and isoprene and thus simulated a larger atmospheric SOA burden. For wildfire aerosol we estimate a clear-sky global annual mean DRE of –0.06 W m$^{-2}$ and an almost zero all-sky annual global mean DRE of –0.01 W m$^{-2}$. This is consistent with *Forster et al.* [2007] who reported a multimodel mean all-sky DRF of 0.03±0.12 W m$^{-2}$ despite clear-sky negative forcing, an effect attributed to absorption by the black carbon component of wildfire aerosol when present above clouds.

[11] The largest CAEs are calculated for DMS- (–0.76 W m$^{-2}$) and volcanic-derived sulfate (–0.61 W m$^{-2}$), with substantially weaker global mean CAEs from the other natural sources (Table 1). The volcanic CAE we calculate here is slightly larger than in *Schmidt et al.* [2012] because of the larger volcanic emission flux used in our study. The large CAE from DMS and volcanoes occurs because they contribute a large number of small particles which result in a large increase in CDNC per unit of aerosol burden. The larger size of sea-salt particles compared to other natural aerosol sources results in a smaller impact on CDNC per unit of emission and a small CAE (–0.04 W m$^{-2}$) despite the larger atmospheric burden. *Menon et al.* [2002] calculated a substantially larger global mean CAE (–1.82 W m$^{-2}$) despite a similar sea-salt burden to our model because they do not calculate CDNC based on the aerosol size distribution, but use an empirical relationship between aerosol mass and CDNC. In our simulations the presence of large sea-salt particles can also suppress in-cloud supersaturation which can prevent other smaller particles from activating to form cloud droplets [*Rap et al.*, 2009; *Korhonen et al.*, 2010]. The global mean CAE of terpene-derived SOA that we calculate is also relatively small (–0.02 W m$^{-2}$) compared to other natural sources, partly because a positive RE over tropical oceans offsets a continental cooling.
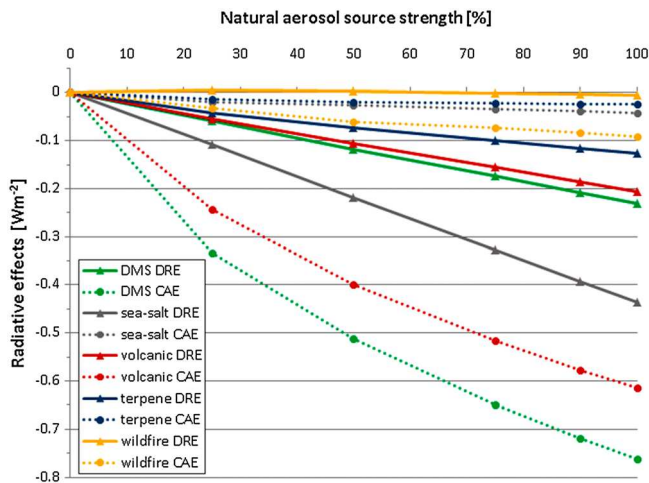
**Figure 2.** Sensitivity of direct (DRE) and cloud albedo effects (CAE) to the natural aerosol source strength in the present-day atmosphere.

Globally, the inclusion of terpene-derived SOA yields an annual mean increase in simulated CDNC, due to the growth of particles in the hydrophilic distribution, and the ageing of particles in the nonhydrophilic distribution. Over some tropical ocean regions nucleation scavenging of the large hydrophilic particles, and subsequent loss through precipitation, dominates over the growth of particles to CCN active sizes, yielding a small decrease in CDNC and a positive indirect RE. *Goto et al.* [2008] calculated an aerosol indirect effect (including cloud albedo, lifetime effects, and semi-direct effects) due to monoterpene SOA of –0.19 W m$^{-2}$, whilst *O'Donnell et al.* [2011] estimated a positive global mean aerosol indirect effect (+0.23 W m$^{-2}$) due to SOA. However, a direct comparison is difficult because *O'Donnell et al.* [2011] included an anthropogenic component to SOA and calculated an aerosol indirect RE that included both the cloud albedo and cloud lifetime effects. Clearly future work is needed to further understand the indirect effect from SOA.

[12] In contrast to the anthropogenic aerosol burden which in the NH is more than four times larger than in the SH, the natural aerosol burden has a relatively larger SH component, mainly due to high sea-salt (SH burden ~90% larger than in the NH) and DMS-sulfate (SH burden ~40% larger than in the NH) loadings, see Figure 1 and Auxiliary Material Figure A1b. While the DRE zonal mean closely matches the burden for all five natural aerosol sources, the CAE is substantially larger in the SH than in the NH due to the large anthropogenic aerosol burden in the PD suppressing the CAE of natural aerosols in the polluted NH [*Chuang et al.*, 2002; *Schmidt et al.*, 2012; *Ward et al.*, 2012]. In the SH oceans the RE is dominated by the DRE from sea-salt and the CAE from DMS sulfate, with zonal mean REs from these sources of up to –0.8 W m$^{-2}$ and –2.8 W m$^{-2}$, respectively. We simulate little seasonal cycle in RE for any of the natural aerosol sources considered except for DMS-derived sulfate where the CAE is significantly larger in the SH summer months (DJF global mean of –1.4 W m$^{-2}$) than in the SH winter months (JJA global mean of –0.29 W m$^{-2}$) due to a strong seasonal cycle of DMS emissions in the SH (see Auxiliary Material Figure A2), consistent with *Thomas et al.* [2010]. During the SH summer, DMS-derived sulfate results in local monthly mean REs of up to –11 W m$^{-2}$ across the Southern Ocean.

[13] Figure 2 shows the RE of the different natural aerosol sources as a function of aerosol source strength. The DRE responds linearly to changes in the emission strength of natural aerosol sources. In contrast, the CAE behavior is nonlinear, due to: (i) CCN number concentrations responding nonlinearly to changes in emissions as a result of aerosol microphysical effects [*Woodhouse et al.*, 2010; *Schmidt et al.* 2012]; (ii) CDNC saturating at high aerosol number concentrations [*Ramanathan et al.*, 2001]; and (iii) cloud albedo responding to the fractional rather than absolute change in CDNC. This results in a unit change in the source strength at lower emission strengths having a larger effect on the CAE than at larger strengths.

[14] There is substantial variability in the aerosol radiative efficiency [*Forster et al.*, 2007] of different natural aerosol sources. Due to the nonlinear CAE, the CAE burden efficiency depends on the magnitude of the perturbation in source strength (Auxiliary Material Table A2). Table 1 details the burden efficiency for the complete removal of each natural aerosol source. In our model DMS sulfate (–616 Wg$^{-1}$), monoterpene SOA (–554 Wg$^{-1}$) and volcanic sulfate (–430 Wg$^{-1}$) have the greatest clear-sky DRE burden efficiencies. There is even larger variability in the CAE burden efficiency with DMS sulfate (–1336 Wg$^{-1}$) and volcanic sulfate (–892 Wg$^{-1}$) efficiencies being up to two orders of magnitude larger than for other natural sources. The DMS sulfate efficiencies for both DRE and CAE are larger than the corresponding volcanic sulfate efficiencies, likely due to the difference in vertical aerosol distributions [*Graf et al.*, 1997]. Also, the ratio of annual global mean CAE to clear-sky DRE in the PD varies between the different natural aerosols from relatively small values for sea-salt (0.06) and terpene SOA (0.18) to larger values for wildfire (1.5), volcanic-sulfate (2.0) and DMS-sulfate (2.2). Aerosol sources that lead to large numbers of small particles (DMS and volcanoes) contribute greatly to CDNC per unit of emission, resulting in a greater CAE burden efficiency.

[15] This is the first study to use the same model framework to quantify the RE for a wide range of natural aerosol sources. Our results typically match previous studies performing similar experiments for specific natural aerosol sources (Table 1), although there are some important differences. In particular, we find that aerosol sources that form large numbers of small particles (DMS and volcanic sulfate) have the greatest impact on cloud albedo. We attribute a substantially smaller CAE to sea-salt than previously estimated [*Menon et al.*, 2002] with potential implications for schemes attempting to modify cloud albedo through the controlled emission of sea-salt particles into the atmosphere [e.g., *Jones et al.*, 2009]. However, we note that the size distribution of naturally emitted sea salt particles is uncertain, with different CAE likely for different sea spray source functions.

[16] We do not study climate-driven perturbations to natural aerosol fluxes, so we cannot explore the role of natural aerosol climate feedbacks such as the CLAW hypothesis [*Charlson et al.*, 1987], the validity of which has recently been questioned [*Quinn and Bates*, 2011]. Specifically, our experiments are different to those by *Woodhouse et al.* [2010], where changes in the global mean DMS-flux of between –20% and +70% resulted in small changes in CCN in the PD. Nevertheless, our results do show that the

RE efficiency of natural aerosol sources can be comparable to that from anthropogenic aerosol sources. Our work implies that we need to better quantify natural aerosol and aerosol-precursor fluxes and better understand their effectiveness in forming CCN. The implications of climate-driven perturbations to natural fluxes, such as the large (+150%) change in regional DMS flux suggested by *Cameron-Smith et al.* [2011] need further investigation.

[18]  The Editor thanks two anonymous reviewers for their assistance in evaluating this paper.

# References

Andreae, M. O., and D. Rosenfeld (2008), Aerosol-cloud-precipitation interactions. Part 1, The nature and sources of cloud-active aerosols, *Earth-Sci. Rev.*, *89*, 13–41.

Bellouin, N., et al. (2013), Impact of the modal aerosol scheme GLOMAP-mode on aerosol forcing in the Hadley Centre Global Environmental Model, *Atmos. Chem. Phys.*, *13*, 3027–3044.

Bowman, M. J. S., et al. (2009), Fire in the Earth System, *Science*, *324*, 481.

Cameron-Smith, P., et al. (2011), Changes in dimethyl sulfide oceanic distribution due to climate change, *Geophys. Res. Lett.*, *38*, L07704, doi:10.1029/2011GL047069.

Carslaw, K. S., et al. (2010), A review of natural aerosol interactions and feedbacks within the Earth system, *Atmos. Chem. Phys.*, *10*, 1701–1737.

Charlson, R. J., et al. (1987), Oceanic phytoplankton, atmospheric sulfur, cloud albedo and climate, *Nature*, *326*, 655–661.

Chuang, C. C., et al. (2002), Cloud susceptibility and the first aerosol indirect forcing: Sensitivity to black carbon and aerosol concentrations, *J. Geophys. Res.*, *107*(D21), 4564, doi:10.1029/2000JD000215.

Dentener, F., et al. (2006), Emissions of primary aerosol and precursor gases in the years 2000 and 1750 prescribed data-sets for AeroCom, *Atmos. Chem. Phys.*, *6*, 4321–4344.

Edwards, J. M., and A. Slingo (1996), Studies with a flexible new radiation code: I. Choosing a configuration for a large scale model, *Q. J. Roy. Meteorol. Soc.*, *122*, 689–720.

Forster, P., et al. (2007), Changes in atmospheric constituents and in radiative forcing, in *Climate Change 2007: The Physical Science Basis*, Cambridge Univ. Press, Cambridge, UK, pp. 131–234.

Gong, S. L. (2003), A parameterization of sea-salt aerosol source function for sub- and super-micron particles, Global Biogeochem, *Cy.*, *17*(4), 1097.

Goto, D., et al. (2008), Importance of global aerosol modeling including secondary organic aerosol formed from monoterpene, *J. Geophys. Res.*, *113*, D07205, doi:10.1029/2007JD009019.

Graf, H., et al. (1997), Volcanic sulfur emissions: Estimates of source strength and its contribution to the global sulfate distribution, *J. Geophys. Res.*, *102*(9), 10,727–10,738.

Guenther, A., et al. (1995), A Global-Model of Natural Volatile Organic-Compound Emissions, *J. Geophys. Res.*, *100*(D5), 8873–8892.

Haywood, J. M., et al. (1999), Tropospheric aerosol climate forcing in clear-sky satellite observations over the oceans, *Science*, *283*, 1299–1303.

Jones, A., et al. (2009), Climate impacts of geoengineering marine stratocumulus clouds, *J. Geophys. Res.*, *114*, D10106, doi:10.1029/2008JD011450.

Kettle, A. J., and M. O. Andreae (2000), Flux of dimethylsulfide from the oceans: A comparison of updated data sets and flux models, *J. Geophys. Res.*, *105*(D22), 26,793–26,808.

Korhonen, H., et al. (2010), Enhancement of marine cloud albedo via controlled sea spray injections, *Atmos. Chem. Phys.*, *10*, 4133–4143.

Mahowald, N., et al. (2011), Aerosol impacts on climate and biogeochemistry, *Ann. Rev. Env. Res.*, *36*, 45–74.

Mann, G. W., et al. (2010), Description and evaluation of GLOMAP-mode: a modal global aerosol microphysics model for the UKCA composition-climate model, *Geo. Mod. Dev.*, *3*, 519–551.

Menon, S., et al. (2002), GCM Simulations of the Aerosol Indirect Effect: Sensitivity to Cloud Parameterization and Aerosol Burden, *J. Atmos. Sci.*, *59*, 692–713.

Nenes, A., and J. H. Seinfeld (2003), Parameterization of cloud droplet formation in global climate models, *J. Geophys. Res.*, *108*(D14), 4415, doi:10.1029/2002JD002911.

Nightingale, P. D., et al. (2000), In situ evaluation of air-sea gas exchange parameterizations using novel conservative and volatile tracers, *Global Biogeochem. Cy.*, *14*(1), 373–387.

O'Donnell, D., et al. (2011), Estimating the direct and indirect effects of secondary organic aerosols using ECHAM5-HAM, *Atmos. Chem. Phys.*, *11*, 8635–8659.

Quinn, P. K., and T. S. Bates (2011), The case against climate regulation via oceanic phytoplankton sulphur emissions, *Nature*, *480*, 51–56.

Ramanathan, V. et al. (2001), Aerosols, *Climate and the Hydrological Cycle, Science*, *294*, 2119.

Rap, A., et al. (2009), Shepard and Hardy multiquadric interpolation methods for multi-component aerosol-cloud parameterisation, *J. Atmos. Sci.*, *66*(1), 105–115.

Reddy, M. S., et al. (2005), Aerosol optical depths and direct radiative perturbations by species and source type, *Geophys. Res. Lett.*, *32*, L12803, doi:10.1029/2004GL021743.

Rossow, W. B., and R. A. Schiffer (1999), Advances in understanding clouds from ISCCP, *B. Am. Meteorol. Soc.*, *80*, 2261–2288.

Schmidt, A., et al. (2012), Importance of tropospheric volcanic aerosol for indirect radiative forcing of climate, *Atmos. Chem. Phys.*, *12*, 7321–7339.

Schulz, M., et al. (2006), Radiative forcing by aerosols as derived from the AeroCom present-day and pre-industrial simulations, *Atmos. Chem. Phys.*, *6*.

Spracklen, D. V., et al. (2011a), Global cloud condensation nuclei influenced by carbonaceous combustion aerosol, *Atmos. Chem. Phys.*, *11*, 9067–9087.

Spracklen, D. V., et al. (2011b), Aerosol mass spectrometer constraint on the global secondary organic aerosol budget, *Atmos. Chem. Phys.*, *11*, 12109–12136.

Stier, P., et al. (2005), The aerosol-climate model ECHAM5-HAM, *Atmos. Chem. Phys.*, *5*, 1125–1156, doi:10.5194/acp-5-1125-2005.

Thomas, M. A., et al. (2010), Quantification of DMS aerosol-cloud-climate interactions using the ECHAM5-HAMMOZ model in a current climate scenario, *Atmos. Chem. Phys.*, *10*, 7425–7438.

van der Werf, G. R., et al. (2004), Continental-scale partitioning of fire emissions during the 1997 to 2001 El Nino/La Nina period, *Science*, *303*(5654), 73–76.

Ward, D. S., et al. (2012), The changing radiative forcing of fires: global model estimates for past, present and future, *Atmos. Chem. Phys.*, *12*, 10857–10886.

Woodhouse, M. T., et al. (2010), Low sensitivity of cloud condensation nuclei to changes in the sea-air flux of dimethyl-sulphide, *Atmos. Chem. Phys.*, *10*, 7545–7559.